Review Article

Recycling of the Al Scrap: The Effect of Adding Inoculant Nb+B and Mg with Subsequent Heat-Treatment in the Mechanical Behavior of Al Alloy

Carlos Narducci Jr[1,2,3]*, Junior N[3] and Abdalla AJ[2]

[1]Aeronautics Institute of Technology-ITA, São José dos Campos, SP, Brazil

[2]Institute for Advanced Studies-IEAv, São José dos Campos, SP, Brazil

[3]Federal Institute of São Paulo-IFSP, Itaquaquecetuba, SP, Brazil

*Corresponding author: Carlos Narducci Junior, Aeronautics Institute of Technology-ITA, São José dos Campos, 1249, Rua Alto Garças, Cidade Patriarca, São Paulo - SP, Brazil

Abstract

A new perspective for the use of Al-Si alloys produced with recycled Al (with Fe>1%) in Gravity Die Casting (GDC) processes. To study the morphology of β-Fe precipitates and the material's mechanical properties were added the inoculate *via* Nb+B and the element Mg with subsequent heat treatment. The samples were cast in Al10Si1Fe0.35Mg alloy in a metal mould according to ASTM B108. The microstructure was analyzed with BSE-SEM and EDS. The work investigated the morphology of β-Fe precipitates and their effects and interactions on the material's mechanical properties. The combined effect resulted in reduced size and shape of β-Fe precipitates, thereby improved higher yield strength (YS = 207.71 MPa), ultimate tensile strength (UTS = 300.35 MPa), and elongation of 4.66%, exceeding the strength and elongation limit values found in commercial alloys, such as ASTM A357 alloy, where the Fe content is low (max. 0.2%).

Keywords: Recycled Al-Si alloys; NbB; Casting; Heat treatment; Mechanical properties; Refinement of the grain; Intermetallic precipitates

Introduction

Even in small amounts, iron (Fe) degrades the mechanical properties of aluminum alloys, such as tensile strength, fatigue, fracture toughness, and especially the material's elongation. The work of Taylor [1] reports the formation of the intermetallic phase β-Al5FeSi (β-Fe), with thick morphology in the form of plate or needle, it becomes rigid points in the soft structure of the material that, when subjected to external stresses, initiate small fissures extend into cracks that eventually decrease its mechanical properties [1]. As a result, recycled Al, due to the contamination of the material with Fe during its production process, is not recommended for applications where resistance and elasticity are required in the same product. Some examples of products with automotive applications that could benefit from this process are Master Cylinders, Calipers, Camshaft Rockers, and Suspension Brackets components, among other automotive and aerospace parts.

Mahta [2] says the commonly accepted method to alleviate the harmful influence of iron is adding one or more corrective elements [2]. Such additions generally convert the β-Fe platelets into α-Fe dendrites. One example of modification mechanisms is adding chemical elements to the alloy, Mn being the most commonly used today. However, Ebhota [3] states that with this mechanism, a new problem can arise with so-called sludge formation, which reduces the material's mechanical properties [3]. Another approach to combat the level of iron impurity in Al alloys is diluting the recycled aluminum using primary aluminum, but this makes the material more expensive. Basak [4] proposed the fragmentation theory as the mechanism for the β phase's refinement, based on experimental evidence. With a suitable heat treatment, one can change the

morphology of the β-phase [4]. However, it is only recommended in recycled Al-Si alloy castings with low Si concentrations and high Fe concentrations, which is not the case for castings made by the gravity die casting process because the Si element is essential for the fluidity material in the mold. BASAK also proposed gravitational segregation, but this is not an economically productive process. Thus, there is a real need to search for a viable alternative to deal with the high iron concentration in recycled aluminum alloys. In this sense, this work studies the simultaneous use of two techniques to enhance the material's strength: the phenomenon of heterogeneous nucleation and precipitation hardening.

Grain reduction through inoculation via chemical elements (heterogeneous nucleation) has been studied for decades. Easton [5] already confirmed that Ti is an element with an excellent growth restriction factor of the α-Al grain, proving that inoculation with the addition of a master alloy Al-Ti-B acts as powerful refiners the production of Al stamping parts [5]. Al alloys for the stamping process generally use quantities lower than 2 Wt.% of Si. However, in the case of Al-Si alloys for casting, studies with much higher Si levels would be necessary to ensure the reliability of the final products. Nowak [6] report that the inoculants' efficiency based on the master alloy Al-Ti-B is doubtful when using Si concentrations higher than 4 Wt.%, proving through microstructural analyzes that Ti and Si interact to form titanium silicates, which are ceramic compounds and end up damaging the alloy's mechanical properties, this phenomenon has been treated as a poisoning effect on the alloy [6]. The same results were reported for Li [7] about understanding grain refining and the anti-Si-poisoning effect [7].

Thus, the alternative found by engineering among the elements

available in the periodic table was Nb as explained in Bolzoni [8], reporting that Nb because it has a higher melting point and a slightly lower network parameter with lower incompatibility than Ti, which favors the solidification of the molten Al [8]. Bolzoni [9,10] report that niobium-based compounds are highly effective in refining α-Al dendrite grains of Al-Si cast alloys with silicon levels greater than 6 Wt.% of Si, demonstrating through the underlying mechanism of heterogeneous nucleation the clusters of AlB2 and Al3Nb substrates found in the nucleus of the α-Al grains, being revealed as crystals that grow along a non-specific direction and also without a specific orientation relationship, initiating several nucleation points at the same time, limiting the size of the α-Al grain dendrites [9,10]. This phenomenon causes the refinement of the grain and creates a mechanism that ends up modifying the morphology of intermetallic precipitates. Narducci [11,12] reports that the addition of Nb+B caused an exponential increase of the nucleation points (heterogeneous nucleation), forming a large number of simultaneous grains that ended up restricting the mobility of the solute elements and thus decrease their interconnectivity and also the formation of agglomerates and finally present a refined grain structure with reduced and spheroidal β-Fe intermetallic precipitates [11,12]. Theoretically, the yield strength values are correlated to the grain size α-Al. According to the Hall-Petch equation, the smaller the average grain size, the higher the grain boundaries' density and, therefore, the greater the obstruction to the movement of disagreements. Thus, a larger load will then be required to stimulate disagreements, increasing the yield strength.

Precipitation hardening is a technique used in Al-Si cast alloys generally with a Fe content within the recommended limits (e.g., ASTM A357 alloy) to strengthen the material's mechanical properties. According to Apelian [13], the process consists of adding an alloying element (Mg or Cu) to the material, with the subsequent heat treatment of solubilization and precipitation (T6) [13]. Mcqueen [14] explains that in this heat treatment process, the material is heated within the monophasic region for a sufficient time for solubilization of the solute atoms, followed by quick cooling to obtain a supersaturated solid solution [14]. Then the alloy is reheated at a temperature below the monophasic region to allow for the precipitation of finely dispersed particles from the supersaturated solid solution. The formation of a fine precipitate dispersion hinders discordance's movement.

Experimental Procedure

The materials used were: Primary Al (supplied by HYDRO), Si (supplied by LIASA), Fe (supplied by MEXTRAMETAL), Mg (supplied by RIMA), and an Al4Nb0.05B master alloy (supplied by Companhia Brasileira de Metalurgia e Mineração - CBMM). Manufactured the tensile test standard (TTS) was in the Sunny foundry in Itaquaquecetuba.

The metal was melted in an electric crucible oven with a capacity of 60 kg of material. After adding each element, the temperature was stabilized at 850±10 ºC, with a 1-hour hold was applied to ensure complete dissolution. Degassing was then carried out by adding hexachloroethane tablets (supplied by ALFA TREND). Each sample collection, achieved homogenization by 30 s of stirring and a new temperature stabilization at 720±10 ºC, followed by a second homogenization at the same temperature, with 30 s of stirring and

Table 1: Chemical composition of TTS.

Batch	Elements (Wt. %)					
	Al	Si	Fe	Nb	B	Mg
1º	balance	10	1	0	0	0
2º	balance	10	1	0.05	0.00625	0
3º	balance	10	1	0.05	0.00625	0.35
4º	balance	10	1	0	0	0.35

sample collection. The chemical composition of each batch produced is shown in Table 1. The verification of the base alloy was done by atomic absorption spectrometry.

The casting was done by the gravity Die Casting Process (GDC), using a metallic mold (supplied by Alpha Trend), manufactured according to the ASTM B108 standard, 2018. The heat treatment (T6) was carried out in a muffle furnace located in the metallurgy laboratory of ITA. The T6 heat treatment parameters used were: temperature of 535±5 ºC, duration of 4 h±15' (solubilization), transferred immediately to a water tank at room temperature (25 ºC) for 15 minutes (quenching). Then, the TTS group was heated at a temperature of 175±5 ºC, a duration of 7 h±15' (precipitation or artificial aging), with subsequent cooling in the open air. Figure 1 shows the curve with the treatment route applied in the process for the intended specific precipitation (T6).

To analyze the grain size, it took the samples' cross-sectional surfaces from the central body of the TTS, cut in the horizontal and vertical directions when filling the piece, prepared with 2400 mesh sandpaper sheets without polishing. After the metallurgical preparation, attacked the samples for 15 seconds with a Poulton acid solution. For the analysis of the microstructural constituents, the cross-section surfaces, after being prepared with 2400 mesh sandpaper sheets, were polished with a 1μm alumina suspension and then chemically attacked with the Keller reagent. The macro and microstructures were examined in an optical microscope with polarized light, filter plate, and Differential Interference Contrast (DIC). The measurement of the average grain size (G) was conducted by the linear intercept method according to the ASTM E112-10 standard, 1996. The β-Fe intermetallic precipitate was analyzed by X-ray Dispersive Energy Spectroscopy (EDS) with a Tescan scanning electron microscope from Oxford Instruments.

X-ray diffractometry (XRD) tests were performed on the samples in a Seifert URD65 diffractometer with Co-Ka radiation. For
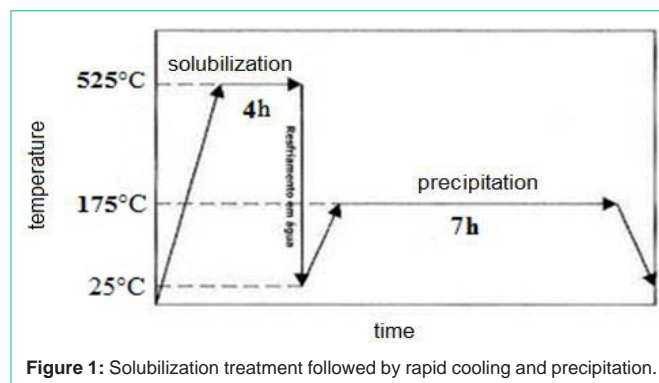

Figure 1: Solubilization treatment followed by rapid cooling and precipitation.
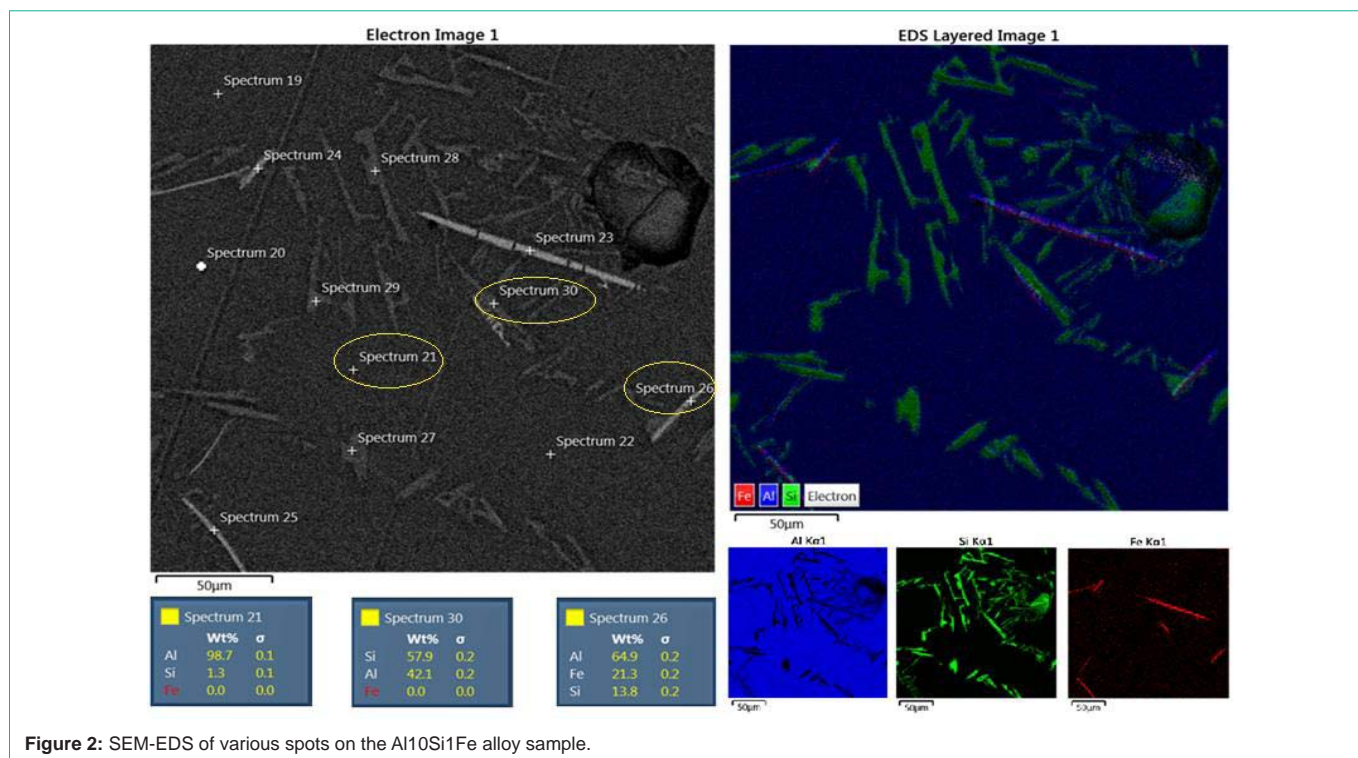
Figure 2: SEM-EDS of various spots on the Al10Si1Fe alloy sample.

indexing the diffraction peaks, the HighScore program from Malvern Panalytical was used with the Inorganic Crystal Structure Database (ICDS).

The tensile test was performed in a universal machine (brand Quanteq), model Emic Trd28 and equipped with a TestScript304 software for testing methods, located in the metallurgy laboratory of the Federal Institute of São Paulo (IFSP) - Campus Itaquaquecetuba. The data obtained were: Yield Strength (YS), Ultimate Tensile Strength (UTS), and elongation (%). Three CDPs were tested for each batch of material according to the chemical composition detailed in Table 1, without and with the addition of Nb+B, Mg, and subsequent heat treatment (T6), with five test conditions, as follows:

- Base material;
- Base material with added Mg and T6;
- Base material with added Nb + B;
- Base material with the addition of Nb + B and T6;
- Base material with added Mg, with added Nb + B and T6.

Results and Discussion

In a first analysis, the sample characterization, the a-Al grain size, and the morphology of the b-Fe precipitate were checked. Then the mechanical behavior of the alloy was studied.

Figure 2 shows the images in the SEM-EDS characterizing of the Al10Si1Fe alloy, by chemical analysis of the spectra, with point 21 being composed of aluminum; points 29 and 30 are composed of 8.9% Al and 91.1% Si, 57.9% Al, and 42.1% Si, by weight, respectively, in the proportion of the chemical composition expected for eutectic silicon; and point 26 is composed of 64.9% Al, 13.8% Si, and 21.3%

Fe, by weight, in proportion to the chemical composition expected for precipitated β-Fe particles.

In this image, you can see the β-Fe precipitates in the form of large, coarse needles that turn out to be hard spots in the material's structure and impair its mechanical properties.

Already in Figure 3 is shown the images in the SEM-EDS characterizing the Al10Si1Fe alloy with the addition of the inoculant Nb+B, where point 49 is composed of aluminum; point 48 is composed of 20.9% Al and 78.9% Si, in the proportion of the chemical composition expected for eutectic silicon; point 40 is composed of 65.7% Al, 16.0% Si, and 18.3% Fe, by weight, in the ratio of chemical composition expected for precipitated β-Al5FeSi (β-Fe) particles; and point 47 is composed of 72.6% Al and 27% Nb, by weight, in the ratio of chemical composition expected for Al3Nb particles.

The precipitated particles of β-Al5SiFe (β-Fe) are characterized by small and spheroidal particles with homogeneous distribution, along with the eutectic Si. Besides these particles, there are Al3Nb particles distributed in the material. The NbB2 particles are smaller particles that do not allow a quantitative point analysis.

With the magnification of 12000 X, it was possible to see in Figure 4a, the Al3Nb and NbB2 substrates found in the Al4Nb0.5B master alloy. In Figure 4b, shows the XRD of the Al4Nb0.05B master alloy, confirming the substrates' presence added to the material. These substrates remain stable after casting the alloy. This process is described in the literature as a solid particle, which is still in the liquid phase when placed in contact with the substrates (Al3Nb or NbB2), "wets," i.e., spreads and covers the surface, causing the necessary undercooling for grain nucleation [15]. These substrates responsible for heterogeneous nucleation in the material initiate
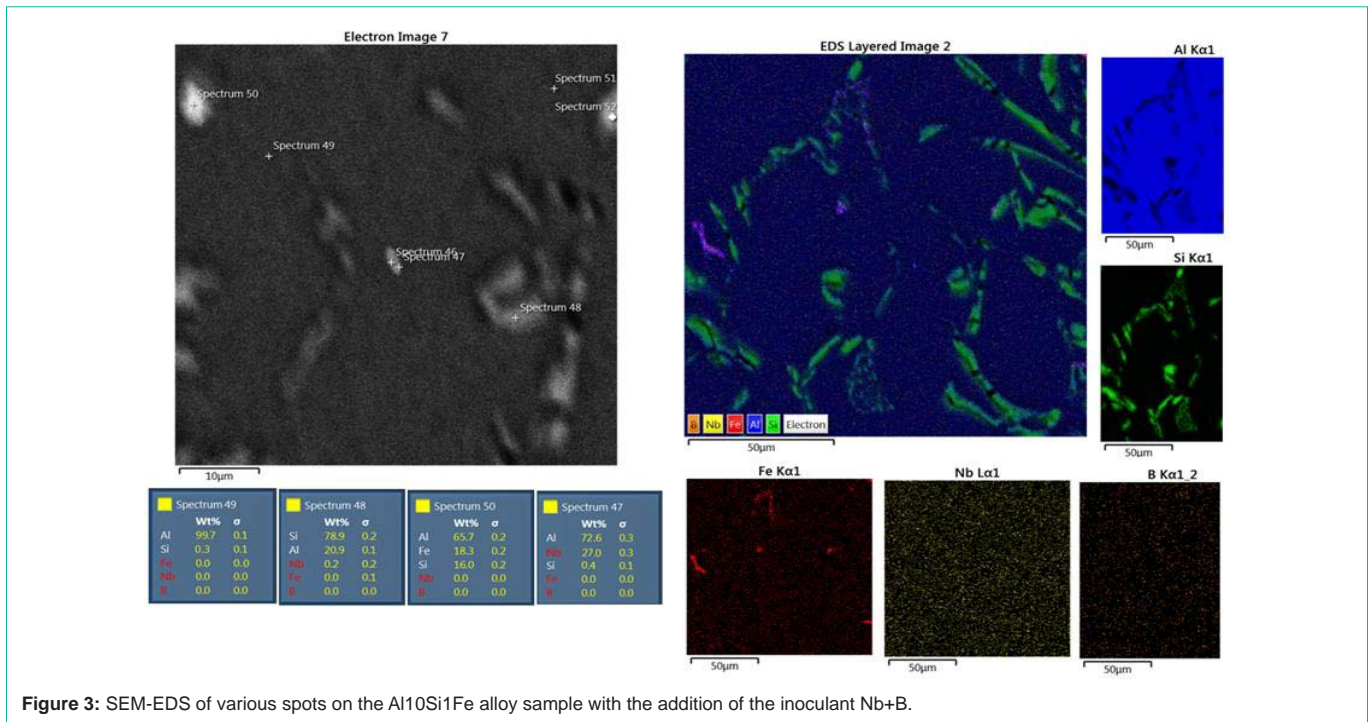
Figure 3: SEM-EDS of various spots on the Al10Si1Fe alloy sample with the addition of the inoculant Nb+B.
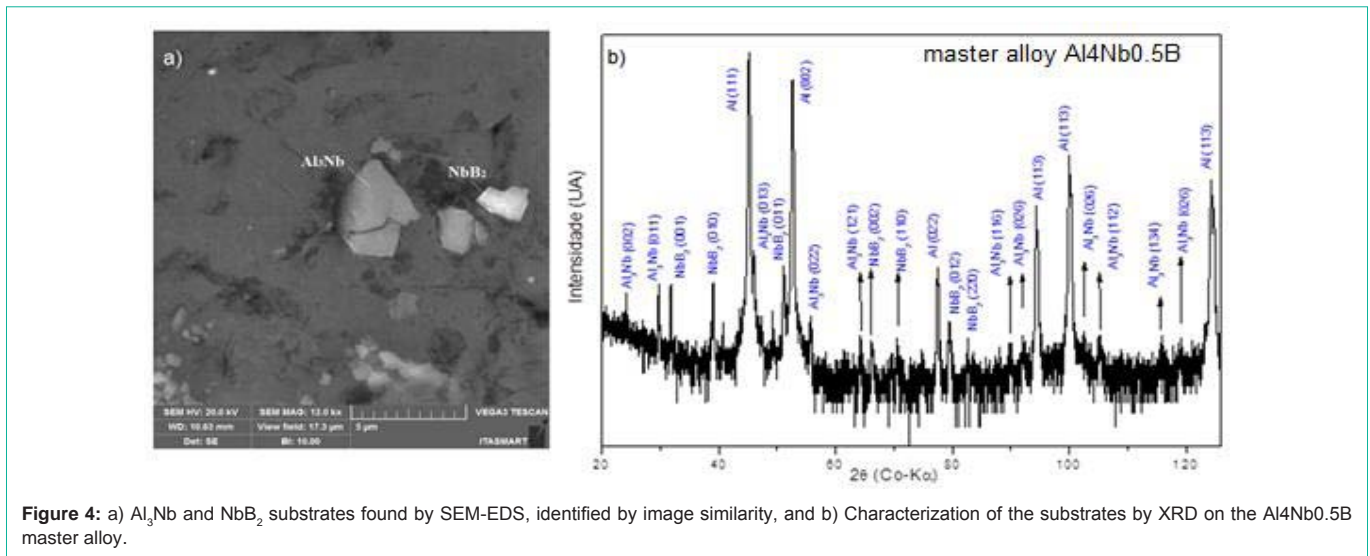

Figure 4: a) Al_3Nb and NbB_2 substrates found by SEM-EDS, identified by image similarity, and b) Characterization of the substrates by XRD on the Al4Nb0.5B master alloy.

several simultaneous nucleation points promoting the refinement of α-Al grains.

Figure 5 shows the size of the α-Al grains.

The average grain size (G) measurement was conducted by counting the number of grains intersecting a line of known size. The grains were numbered in ascending order from left to right. Figure 6 exemplifies the methodology used, with the lines drawn and the number of grains intercepting each line (shown at its end).

Overall the reduction in average grain size was 438% (from 96μm to 221μm) compared to the base alloy without the addition of the inoculant. The Works of Xu [16-18] bring the development of Al-Nb-B master alloy with a high Nb/B ratio for grain refinement where

was the in-situ observation of grain refinement dynamics and the effect of Agglomeration on Nucleation Potency of Inoculant Particles in the Al-Nb-B Master Alloy [16-18]. The results were in the same line as found in this work.

Besides causing grain refinement, this phenomenon also creates a mechanism that modifies the morphology of the β-Fe precipitates. Figure 7 shows the difference in morphology and size of the β-Fe precipitates by SEM images. The spectra of β-Fe are highlighted by light gray color, being in the samples without addition of the inoculant of elongated and large shape, as can be seen in Figure 7a and 7b and in the samples with addition of the inoculant Nb+B, the precipitates of β-Fe, present spheroidal shape, and reduced size, as shown in Figure 7c, 7d.
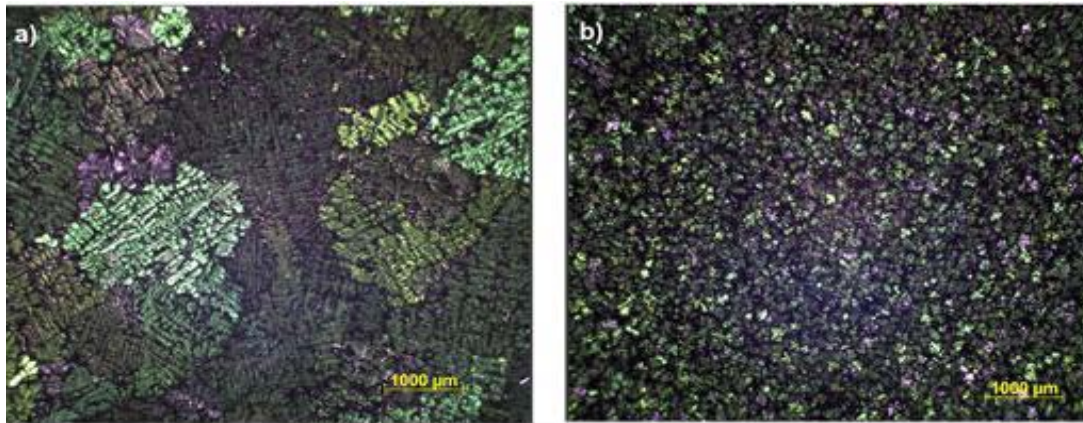
Figure 5: Primary α-Al grain size. a) without addition and b) with the inoculant Nb+B (0.05 Wt.% Nb).
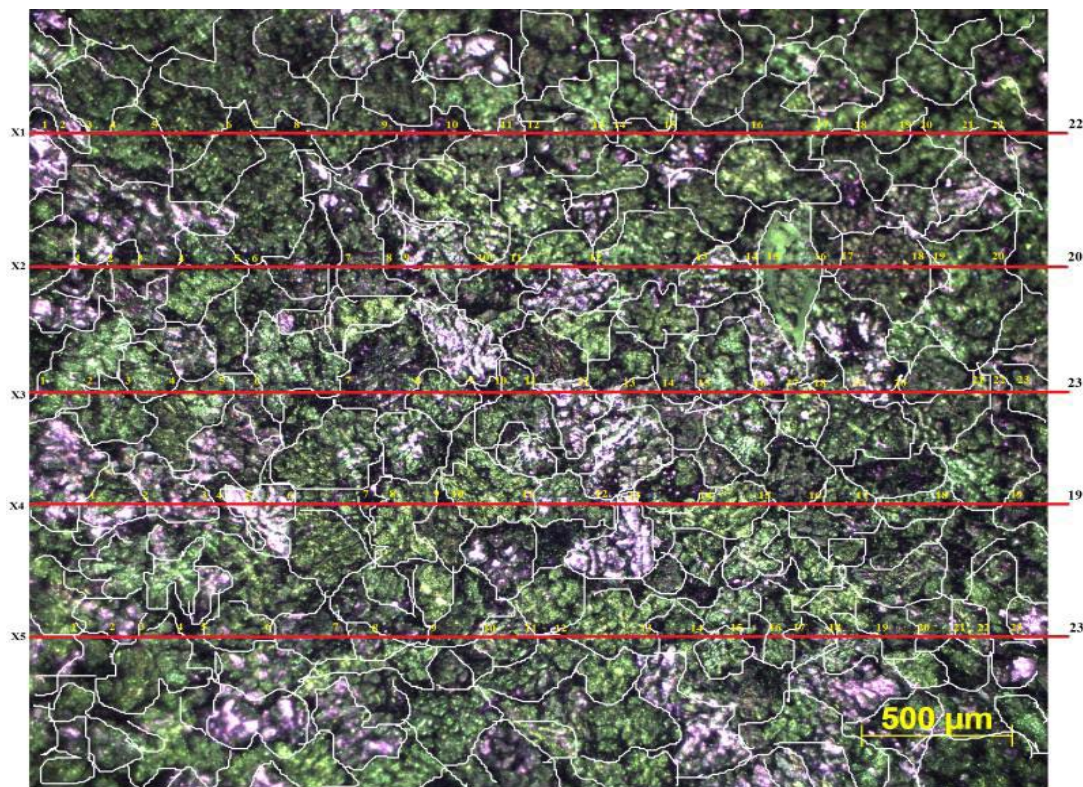

Figure 6: Example of counting the intercepts for grain size determination in Al10Si1Fe alloy with Nb+B.

It is worth noting that this drastic reduction in the size of the eutectic structures and intermetallic precipitates was achieved at a slow cooling rate. With this condition, it is very hard to obtain the ''modification'' of the needle-shaped eutectic phase and intermetallic precipitates of β-Fe from their thick plate shape to reduced size and spheroidal morphology. This is a highly desirable condition of the material structure.

The analysis of Figure 7 showed the drastic reduction in the size of the β-Fe intermetallic precipitates and practically the extinction of microporosity points in the material structure, eliminating the possibility of crack initiation when the material is subjected to mechanical stress.

By studying the morphology of the β-Fe particles, changes in the size of the precipitates were found, leading to reduced and scattered particles in the material structure, as can be seen in Figure 7c,7d. This reduction may be happening due to the evolution of liquid Al during its solidification. The solute elements (Si and Fe) are expelled from the primary α-Al grains until the concentration of the eutectic phase (12.6% by weight of Si) is reached, where the Fe particles have precipitated together with the eutectic Si. Since any solidification event takes place by nucleation and growth, it can be proposed that with nucleation at the several simultaneous points of the α-Al
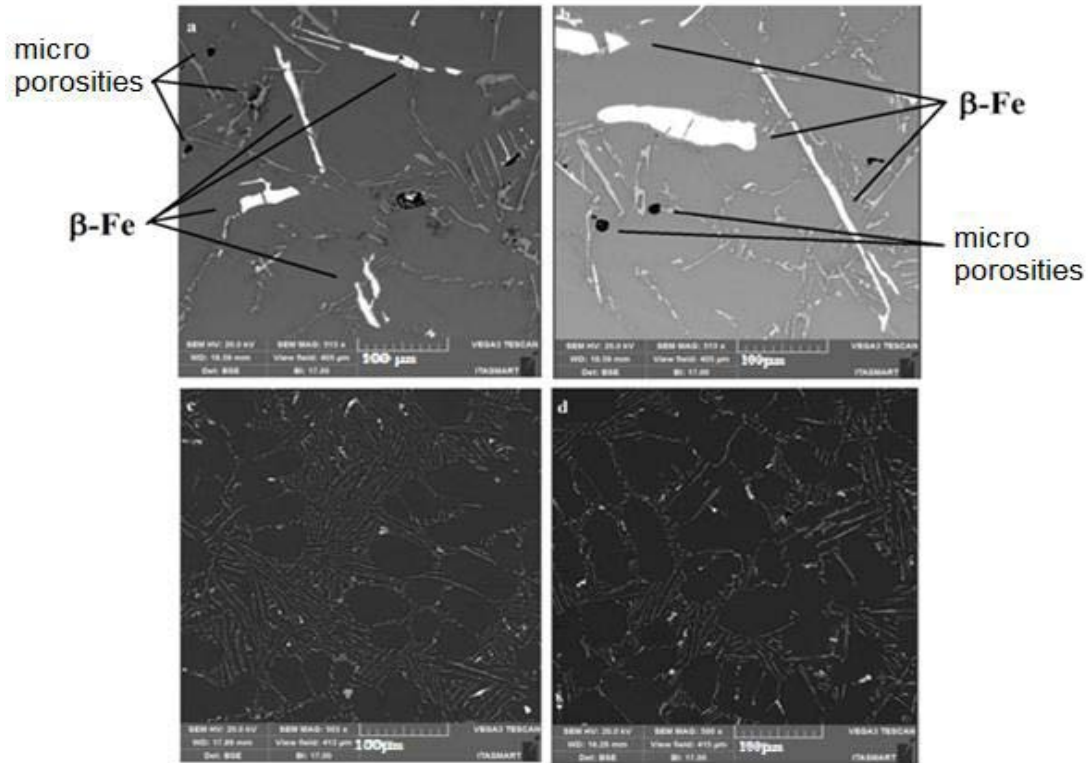
Figure 7: Image (a and b) showing the morphology of β-Fe spectra (light gray) of elongated and large shape with scattered microspores in the material structure, before the addition of Nb+B and image (c and d) showing the morphology of β-Fe spectra (light gray) of spheroidal shape and reduced size and with pore-free material structure, after the addition of Nb+B.
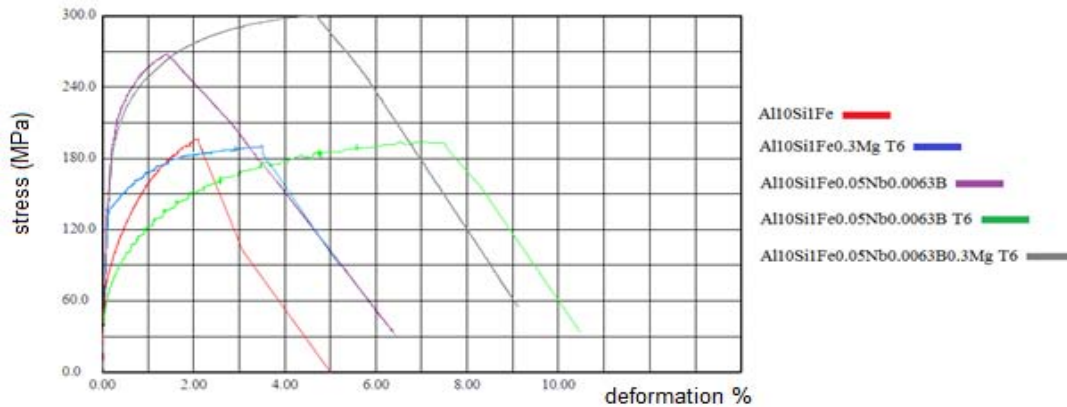

Figure 8: The tensile strength as a function of elongation for the cast lots. Base material (red curve); With the addition of the Mg element and T6 (blue curve); With the addition of Nb+B (lilac curve); With the addition of Nb+B and T6 (green curve); With the addition of Nb+B, the Mg element, and T6 (gray curve).

dendritic grains (heterogeneous nucleation), the solute rejected at the solidification front and in the eutectic pools, but now trapped between the several, reduced dendritic arms of the Al grains, end up having no approximations, clusters or interconnectivity between the partner solute elements. I.e., the concentration gradient of the same element was reduced for the growth of the second phase precipitates, consequently reducing the size of the precipitated particles, which due to the more homogeneous distribution of the solute elements dispersed in the material, gave a new dynamic to the formation mechanism of the β-Fe precipitates. An investigation carried out by

Taylor [1] noted an increased tendency to form porosity at high iron levels [1]. However, the inoculant Nb+B addition showed a reduction in micro porosities as per Figure 7c,7d. The micro porosities are caused by the oxide films in the liquid metal. Theoretically, these films also act as a substrate for nucleation of β-Fe intermetallic phase formation. Therefore, without the micro porosities, it is expected that fewer β-Fe precipitates will be formed in the material.

Tensile tests were performed to study the mechanical behavior of the material on the CDPs before and after the heat treatment (T6).

Table 2: Shows a summary table comparing the results achieved for the five types of specimens tested.

| Batch	Change in chemical composition and heat treatment T6			Variations produced in the tens ile properties		
	0.05%Nb + 0.0063%8	0.35% MG	Again T6	YS	UTS	elongation
Base Material (MB)	-	-	-	Reference (96 Mpa)	Reference (197 Mpa)	Reference (2.1%)
MB+NbB	yes	-	-	124% (215 Mpa)	36% (268 Mpa)	-14% (1.8)
MB+NbB+T6	yes		yes	-19% (78 Mpa)	-1% (194 Mpa)	262% (7.6)
MB+Mg+T6		yes	yes	50% (143 Mpa)	-3% (191 Mpa)	71% (3.6)
MB+NbB+Mg+T6	yes	yes	yes	117% (208 Mpa)	53% (300 Mpa)	124% (4.7)
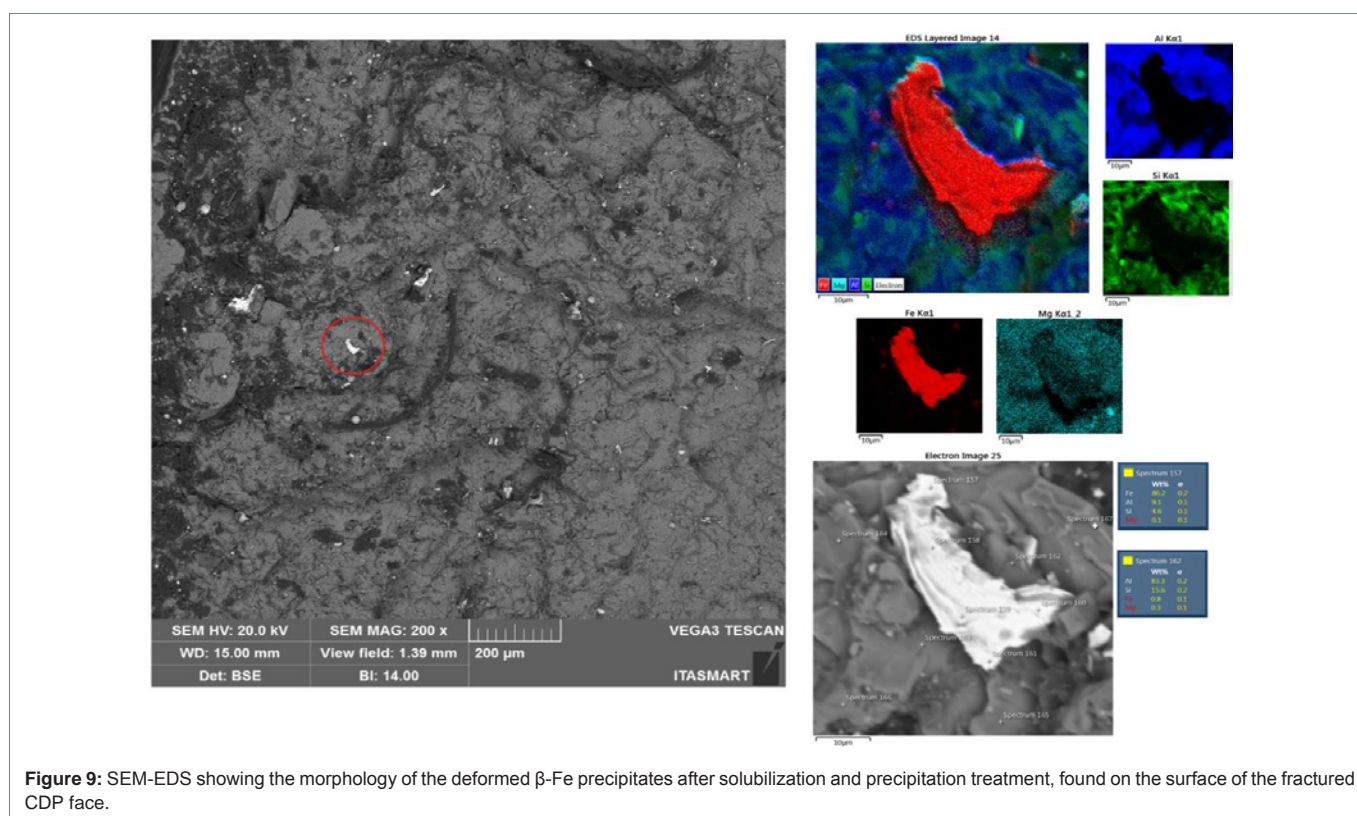
Figure 9: SEM-EDS showing the morphology of the deformed β-Fe precipitates after solubilization and precipitation treatment, found on the surface of the fractured CDP face.

The results were tabulated as shown in Table 2.

The graph in Figure 8 shows the Stress X Strain curves for each type of sample evaluated.

The explanation of the results of the base material (red curve), with the material with the addition of the Mg element and with the T6 treatment (blue curve), is due to the presence of the particles of β-Fe coming from the Fe-critical with morphology in the form of plates or coarse needles, as shown in Figures 7a,7b - without the addition of Nb+B, which ultimately impacts the strength limit of the material. Bacaicoa [19] reports that after the solubilization and precipitation heat treatment, the β-Fe particles are found with distorted and decomposed morphology [19]. As observed on the broken face of the tensile specimens, the images are shown in Figure 8 distorted and decomposed morphology results in a more ductile fracture mode and an increase in material elongation (Figure 9).

The Mg_2Si precipitate, formed with the addition of the Mg element

in the alloy, forms solubilized and finely dispersed particle precipitates, serving as a reinforcement mechanism for the material in its elastic region, which justifies the increased yield strength found. However, when the deformation of the material enters the plastic region, with the increase in stress, the β-Fe particles, although deformed, are still rigid points in the structure of the material. Furthermore, one should also observe the micro porosities arising from the Fe-criticality in the alloy. In these regions, cracks started, which eventually embrittled and limited the maximum strength of the material. Thus, signaling that the heat treatment (T6) has no beneficial effect on the strength limit (UTS) in alloys with Fe-critical.

The explanation of the results with the base material (red curve), with the material with the addition of the inoculant Nb+B (purple curve), can be understood due: The increase in the yield strength of the material and the strength limit can be explained due to the reduced grains with the inoculation *via* Nb+B, brought a greater amount of grain boundaries, the grain boundaries are discontinuities
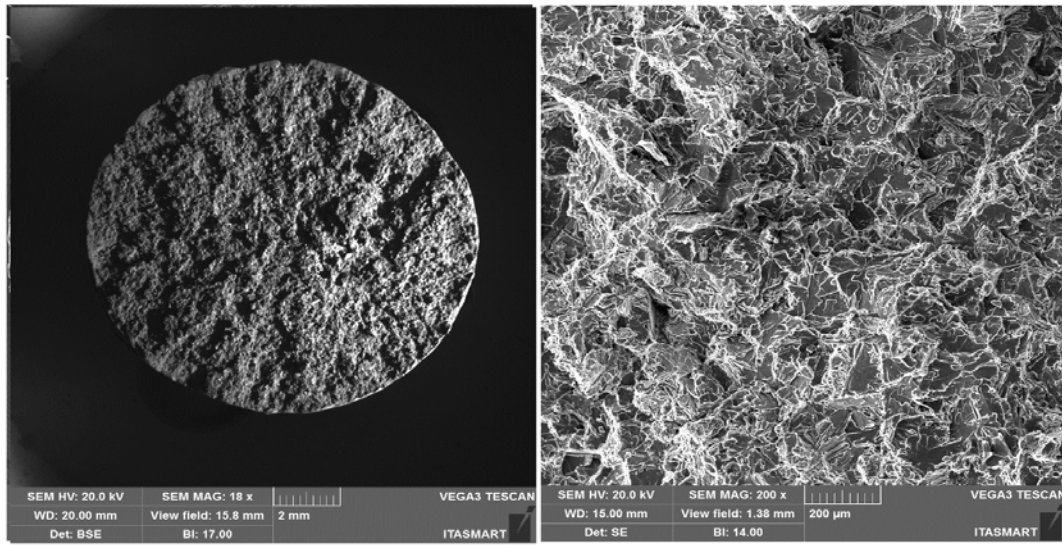
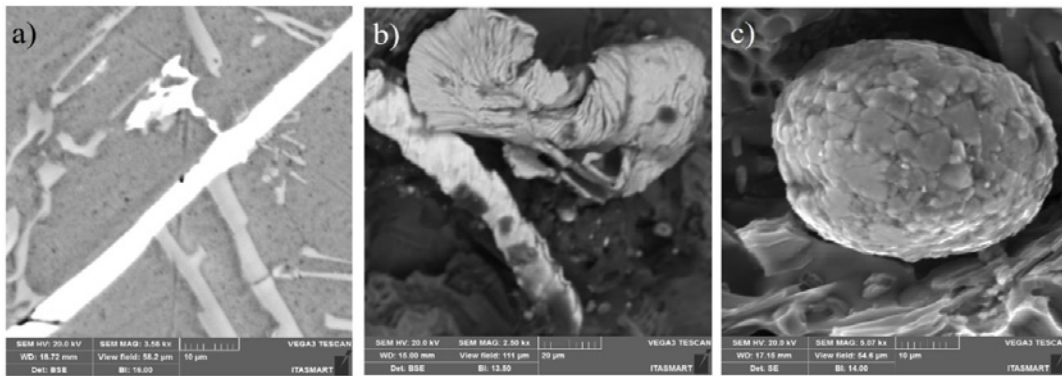**Figure 10:** Fractured CDP face of sample Al10Si1Fe+NbB.

Figure 11: Evolution of the β-Fe precipitated particle. a) precipitates in primitive form. b) precipitates after heat treatment. c) precipitates after grain refinement and heat treatment.

that hinder the movement of disagreements, improving the strength of the material. It should be noted that the α-Al grain inoculation via Nb+B caused a casting structure with not only equiaxial and reduced grain sizes but also a structure without coarse plates of β-Fe particles and no presence of micro porosities, as verified in Figures 7c,7d - with Nb+B, which also contributes to the improved strength of the material. Especially in hypoeutectic alloys (with Si content below 12.7%), the α phase is the continuous phase in the microstructure and is the phase determining the mechanical properties of these alloys. The β-phase is essentially formed by silicon and second phase precipitates, such as β-Fe. Since the mechanical properties of the alloy arise from the mixture between these phases, i.e., in dendrite regions, the mechanical properties are similar to those of the α phase. In contrast, in eutectic regions, the α phase is the continuous phase but intercut by the β phase. The presence of the β phase distributed over the α phase matrix raises the hardness, yield strength, and tensile strength of the alloys but drastically reduces the ductility. On the fractured face of the CDP, it was observed that the rupture shows aspects of a brittle material, as per Figure 10. They were suggesting that the smaller grains made the material stiffer. They were signaling that only the addition of the inoculant Nb+B was not enough to achieve the mechanical properties of elongation desired to the material with Fe-critical.

The explanation of the results with the base material (red curve), with the material with added Nb+B and heat treatment (green curve), can be understood due: It is known that the production of parts with high ductility requires obtaining microstructures without the presence of elongated second phase particles and micro porosities, as is the case of CDPs inoculated via Nb+B, with the second phase particles reduced and spheroidal, the   was improved. Similar results were also found in the work of Novak [20]. With this, plastic deformation started at a lower strain level but extended to about 7.6% strain. Although the precipitation treatment was performed on the CDPs, it did not promote the hardening effect, with the formation of precipitates consistent with the α phase matrix. With the high temperature and long treatment time, there was a greater tendency for grain growth. With this, the material behavior remained similar to the base material regarding the strength limit.

Although these characteristics are interesting for some mechanical applications, the addition of Nb+B, with subsequent TT, without the

Table 3: Comparison between the studied alloy and the A 357 alloy (commercial alloy).

Material	Strength (Mpa)		Elongation (%)
	ultimate	yield	
Al10Si1Fe0.3Mg- with NbB e T6	300.35	207.71	4.66
Alloy 357*	285	215	3.0

*Standard Specification for Aluminum-Alloy, ASTM B108/B108M-Table 1 (no location designated) Table 3.

addition of the Mg element, did not have the reinforcement due to the aluminum matrix and neither the effect in raising the desired strength levels for the cast Al-Si alloy with Fe-critical. The Mg element was introduced to achieve higher strength levels, and the aging treatment was performed, as shown in the gray curve.

During the grain refinement and solubilization treatment, the silicon and iron particles change their morphologies. Fuoco [21] showed in his research that initially, continuous particles undergo a process of fragmentation and rounding (spheroidal) of individual particles [21]. This was confirmed in this research, as shown in Figure 11. An example of the evolution in the morphology of the β-Fe precipitates found in the samples analyzed in the various conditions studied is shown: Figure 11a Al10Si1Fe alloy, β-Fe precipitates in primitive form, Figure 11b Al10Si1Fe0.35Mg + (T6), deformed β-Fe precipitates after heat treatment; and Figure 11c, Al10Si1Fe0.35Mg+NbB + T6, with spheroidal Fe precipitates after grain refinement and heat treatment.

When the Mg element was added to the alloy refined with Nb+B, and after the solubilization and precipitation heat treatment (T6), as shown in the gray curve, there was an increase in all levels of mechanical properties of the material when compared to the base alloy (red curve). It was revealed that the refinement promoted by the addition of the Nb+B inoculant did not alter the precipitation hardening mechanism of Mg_2Si. Likewise, the solubilization of the material did not harm the morphology of the reduced and spheroidal β-Fe particles. Thus, the beneficial actions of the two techniques used for strengthening the material's mechanical properties added up, providing strength and elasticity to the material, properties that are sought after in engineering applications.

Table 3 shows a comparison of the strength and elongation values between the studied alloy and the A357 alloy (a commercial alloy used in engineering applications, with low Fe content, less than 0.2% by weight).

Although the mechanical properties of A357 are minimum values for safety reasons when used in projects, the results of mechanical properties obtained with the studied alloy Al10Si1Fe0,3Mg, inoculated *via* NbB, surpassed those of A357 alloy, suggesting the possibility of using alloys coming from recycling (Fe-critical), for the production of structural and safety parts.

Conclusion

The refinement promoted by adding the inoculant Nb + B did not alter the precipitation hardening mechanism of Mg2Si. Similarly, the solubilization of the material did not harm the morphology of the reduced and spheroidized β-Fe particles. Thus, the beneficial actions of the two techniques used for strengthening the mechanical properties of the material added up, providing strength and elasticity to the material, there was an improvement in yield strength (117%), tensile strength (53%), and elongation (124%) when compared to the base cast alloy (Al10Si1Fe). The comparison of the tensile test results of Al10Si1Fe0,35Mg alloy with Nb+B addition and T6 treatment, with the ASTM A357 market alloy (low Fe content alloy, used for products that require high performance), showed that the former has similar yield strength and superior tensile and elongation limits, and is, therefore, a strong indication for the continuity of the research on alloys coming from recycling (Fe-critical).

Acknowledgments

References

1. Taylor JA. Iron-containing intermetallic phases in Al-Si based casting Alloys. ELSEVIER, Procedia Materials Science. 2012; 1: 19-33.

2. Mahta M, Emamy M, Cao X, CampbelL J. Overview of α-Al5FeSi Phase in Al-Si Alloys; Materials Science Research Trends - Chapter 5; Nova Science Publishers. 2007.

3. Ebhota WS, Jen T-C. Intermetallic Formation and Their Effect on Mechanical Properties of Al-Si-X Alloys. 2018.

4. Basak CB, Babu NH. Morphological changes and segregation of β-Al9Fe2Si2 phase: A perspective from better recyclability of cast Al-Si alloys, BCAST, Brunel University London, Kingston Lane, Uxbridge, Middlesex UB8 3PH, Materials and Design, UK, 2016.

5. Easton M, John D. An analysis of the relationship between grain size, solute content, and the potency and number density of nucleant particles. Metall Trans A. 2005; 36: 1911-1920.

6. Nowak M, Bolzoni L, Babu NH. Grain refinement of Al-Si alloys by Nb-B inoculation. Part I. Materials and Desigs. 2015; 66: 366-375.

7. Li Y, Jiang Y, Liu B, et al. Understanding grain refining and anti Si-poisoning effect in Al-10Si/Al-5Nb-B system. Journal of Materials Science & Technology. 2021; 65: 190-201.

8. Bolzoni L, Nowak M, Hari Babu N. Assessment of the influence of Al–2Nb–2B master alloy on the grain refinement and properties of LM6 (A413) alloy; Materials Science & Engineering A. 2015; 628: 230-237.

9. Bolzoni L, Nowak M, Hari Babu N. Grain refinement of Al-Si alloys by Nb-B inoculation. Part II: Application to commercial alloys. Materials and Design. 2015; 66: 376-383.

10. Bolzonia L, Babu NH. Engineering the heterogeneous nuclei in Al-Si alloys for solidification control. Applied Materials Today. 2016; 5: 255-259.

11. Narducci CJ, Brollo GL, Siqueira RHM, Antunes AS, Abdalla AJ. Effect of Nb addition on the size and morphology of the β-Fe precipitates in recycled Al-Si alloys; Scientific Reports, Springer Nature. 2021.

12. Narducci CJ, Antunes AS, Abdalla AJ. Effect of the heterogeneous nucleation of the primary α-Al grain via the Al-4Nb-0.5B master alloy in Al-Si alloys with high Fe contents. Materials Research. 2021.

13. Apelian D. Aluminum Cast Alloys: Enabling Tools for Improved Performance. North American Die Casting Association. 2009.

14. Mcqueen JH, Spigarelli S, Kassner ME, Evangelista E. Hot Deformation and

Processing of Aluminum Alloys. CRC Press. 2011.

15. Porter DA, Easterling KE. Phase transformations metals and alloys, Van Nostrand Reinhold Co. 1981.

16. Xu J, Li Y, Hu B, et al. Development of Al-Nb-B master alloy with high Nb/B ratio for grain refinement of hypoeutectic Al–Si cast alloys. Journal of Materials Science. 2019; 54: 14561-14576.

17. Xu J, Li Y, Ma K, et al. In-situ observation of grain refinement dynamics of hypoeutectic Al-Si alloy inoculated by Al-Ti-Nb-B alloy. Scripta Materialia. 2020, 187: 142-147.

18. Xu J, Li R, Li Q. Effect of Agglomeration on Nucleation Potency of Inoculant Particles in the Al-Nb-B Master Alloy: Modeling and Experiments. Metallurgical and Materials Transactions A. 2021: 1-18.

19. Bacaicoa I, et al. 3D Morphology of Al5FeSi inclusions in high Fe-content. Science Direct. Structural Integrity Procedia. 2016; 2: 2269-2276.

20. Nowak M, Yeoh W, Bolzoni L, Hari Babu N. Development of Al-Nb-B master alloys using Nb and KBF4 powders. Materials & Design. 2015; 75: 40-46.

21. Fuoco R. Propriedades mecânicas de peças fundidas em ligas Al-Si. 17º Congresso de Fundição-CONAF 2017; São Paul. 2017.